

In the format provided by the authors and unedited.

Stout camphor tree genome fills gaps in understanding of flowering plant genome evolution

Shu-Miaw Chaw  ^{1,6*}, Yu-Ching Liu¹, Yu-Wei Wu², Han-Yu Wang¹, Chan-Yi Ivy Lin¹, Chung-Shien Wu¹, Huei-Mien Ke¹, Lo-Yu Chang^{1,3}, Chih-Yao Hsu¹, Hui-Ting Yang¹, Edi Sudianto  ¹, Min-Hung Hsu^{1,4}, Kun-Pin Wu⁴, Ling-Ni Wang¹, James H. Leebens-Mack⁵ and Isheng J. Tsai  ^{1,6*}

¹Biodiversity Research Center, Academia Sinica, Taipei, Taiwan. ²Graduate Institute of Biomedical Informatics, College of Medical Science and Technology, Taipei Medical University, Taipei, Taiwan. ³School of Medicine, National Taiwan University, Taipei, Taiwan. ⁴Institute of Biomedical Informatics, National Yang-Ming University, Taipei, Taiwan. ⁵Plant Biology Department, University of Georgia, Athens, GA, USA. ⁶These authors contributed equally: Shu-Miaw Chaw, Isheng J. Tsai. *e-mail: smchaw@sinica.edu.tw; ijtsai@sinica.edu.tw **Open Access** This article is licensed under a Creative Commons Attribution 4.0 International License, which permits use, sharing, adaptation, distribution and reproduction in any medium or format, as long as you give appropriate credit to the original author(s) and the source, provide a link to the Creative Commons license, and indicate if changes were made.

The images or other third party material in this article are included in the article's

Creative Commons license, unless indicated otherwise in a credit line to the material.

If material is not included in the article's Creative Commons license and your intended use is not permitted by statutory regulation or exceeds the permitted use, you will need to obtain permission directly from the copyright holder. To view a copy of this license, visit <http://creativecommons.org/licenses/by/4.0/>.

Supplementary Information

Stout camphor tree genome fills gaps in understanding of flowering plant genome evolution

Shu-Miaw Chaw, Yu-Ching Liu, Yu-Wei Wu, Han-Yu Wang, Chan-Yi Ivy Lin,
Chung-Shien Wu, Huei-Mien Ke, Lo-Yu Chang, Chih-Yao Hsu Hui-Ting Yang, Edi
Sudianto, Ming-Hung Hsu, Kun-Pin Wu, Ling-Ni Wang, Jim Leebens-Mack and
Isheng J. Tsai

I. SUPPLEMENTARY NOTE	3
Assignment of intragenomic synteny blocks into linkage clusters	3
II. SUPPLEMENTARY FIGURES.....	4
Supplementary Fig. 1	4
Supplementary Fig. 2	5
Supplementary Fig. 3	6
Supplementary Fig. 4	7
Supplementary Fig. 5	8
Supplementary Fig. 6	9
Supplementary Fig. 7	10
Supplementary Fig. 8	11
Supplementary Fig. 9	12
Supplementary Fig. 10	13
Supplementary Fig. 11	14
Supplementary Fig. 12	15
Supplementary Fig. 13	16
Supplementary Fig. 14	17
Supplementary Fig. 15	18
Supplementary Fig. 16	19
Supplementary Fig. 17	20
Supplementary Fig. 18	21
Supplementary Fig. 19	22
Supplementary Fig. 20	23

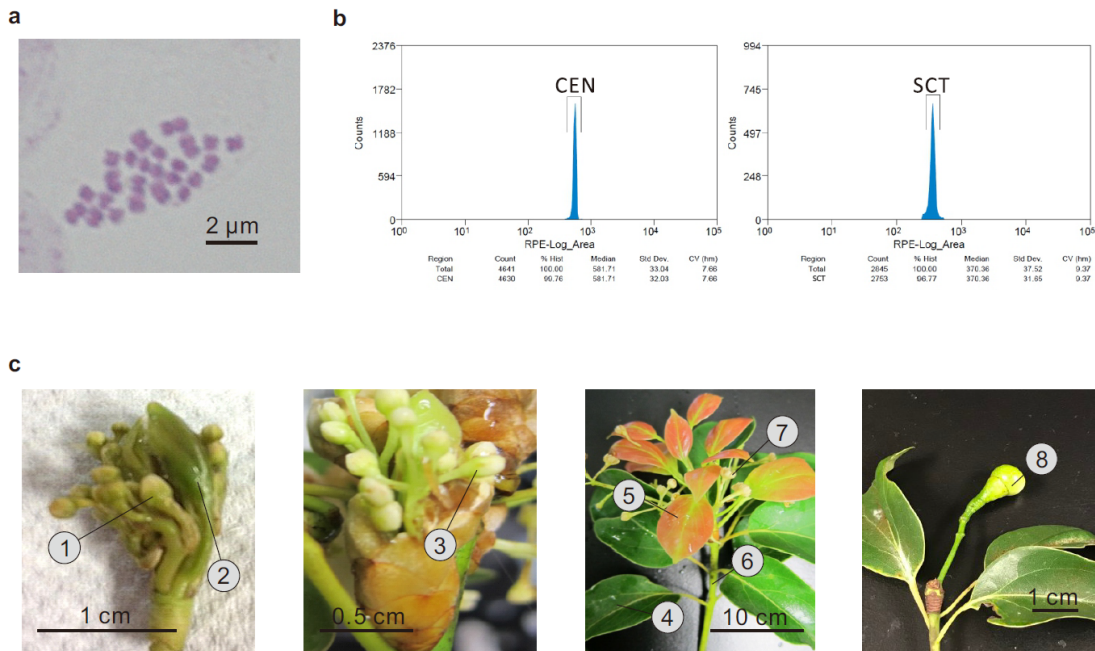
Supplementary Fig. 21	24
Supplementary Fig. 22	25
Supplementary Fig. 23	27
Supplementary Fig. 24	29
Supplementary Fig. 25	30
Supplementary Fig. 26	31
Supplementary Fig. 27	32
Supplementary Fig. 28	33
Supplementary Fig. 29	35
Supplementary Fig. 30	36
III. SUPPLEMENTARY TABLES.....	37
Supplementary Table 1	37
Supplementary Table 2	38
Supplementary Table 3	39
Supplementary Table 4	39
Supplementary Table 5	39
Supplementary Table 6	40
Supplementary Table 7	41
Supplementary Table 8	41
Supplementary Table 9	42
Supplementary Table 10	42
Supplementary Table 11	42
Supplementary Table 12	43
Supplementary Table 13	44

I. SUPPLEMENTARY NOTE

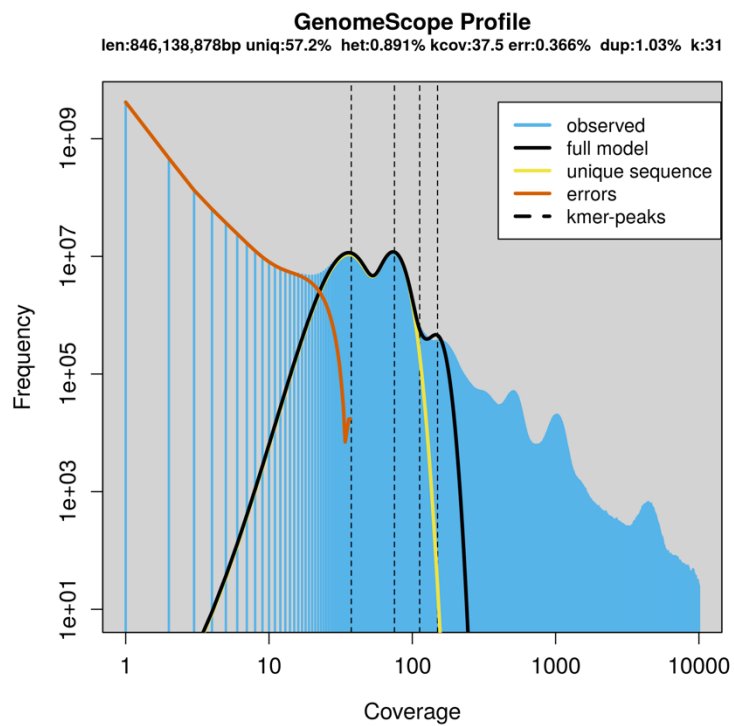
Assignment of intragenomic synteny blocks into linkage clusters

If a genome underwent two rounds of WGD, an ancestral gene may give rise to three paralogous copies and a gene cluster may be syntenic to three other regions. Under this rationale, we categorized all duplicated, triplicated and quadruplicated orthologous genes and regions within synteny blocks as possible signals WGD. Only synteny blocks with more than ten gene pairs defined by DAGchainer¹ was included in this analysis. Synteny blocks that are adjacent to each other in the assembly were merged using Bedtools² and custom python scripts if their corresponding matches were also adjacent to each other. Regions with more than four matches were not considered from this merging process. This resulted 338 synteny blocks with no gap into 81 areas on the longest 12 scaffolds. The merged blocks were then unambiguously classified into linkage clusters by linking the quadruplicated and triplicated orthologues between regions. We repeated this process iteratively to assign the unconnected synteny blocks in proximity to these clusters. Based on these criteria, 55.6% of synteny blocks consisting of 48.0% of the assembly were unambiguously assigned into either group (Supplementary Fig. 13), whilst 36 blocks with the cumulative length of 120.8 Mb were visually inspected and assigned.

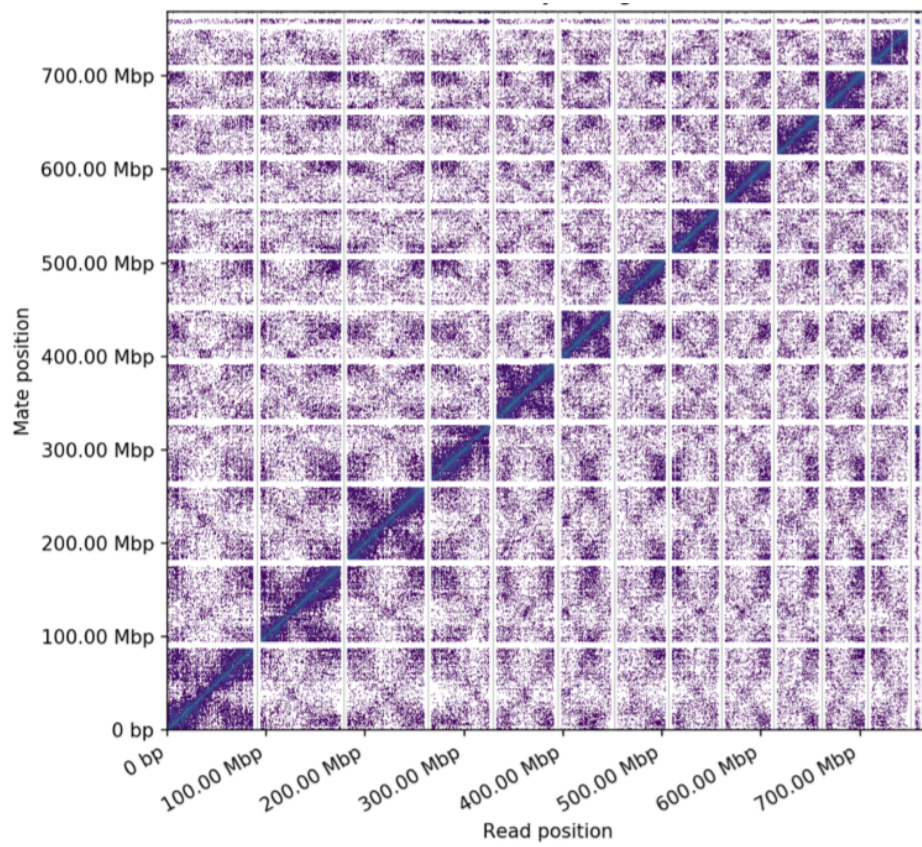
II. SUPPLEMENTARY FIGURES



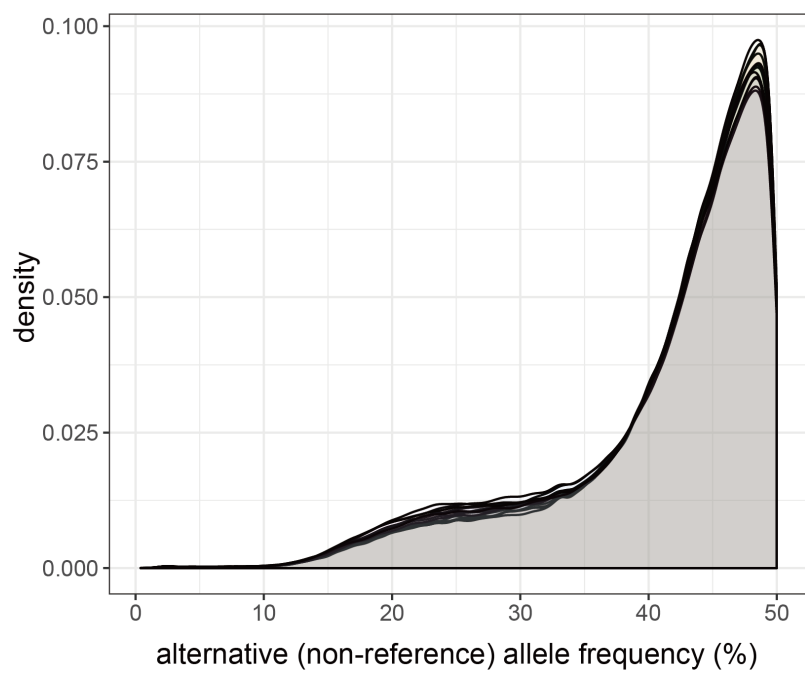
Supplementary Fig. 1. Chromosome biology and transcriptome sequencing of SCT. **a**, Basic fuchsin-stained root tip metaphase cells showing the chromosome number ($2n = 24$). Three independent staining and counts were carried out. **b**, flow cytometry estimation of *C. kanehirae* (SCT: 823.7 ± 58.2 Mb/1C) genome size using chicken erythrocyte nuclei (CEN: 2.5 Gb) as the calibration standard. Two instruments, MoFlo XDP Cell Sorter (Beckman Coulter Life Science, Indianapolis, IN) and Attune NxT Flow Cytometer (Thermo Fisher Scientific Inc., Waltham, MA), were used to measure genome size using single leaf once and twice, respectively. The estimates by using the two instruments were similar and data obtained from the former is shown here. **c**, tissues used for RNA extraction with the stages of (1) flower buds enclosed within inflorescence bracts, (2) immature leaves enclosed within inflorescence bracts, (3) flower buds emerging from bracts, (4) old leaves, (5) young leaves in red, (6) stems, (7) opening flowers, and (8) fruits. Extractions were carried out once for every tissue.



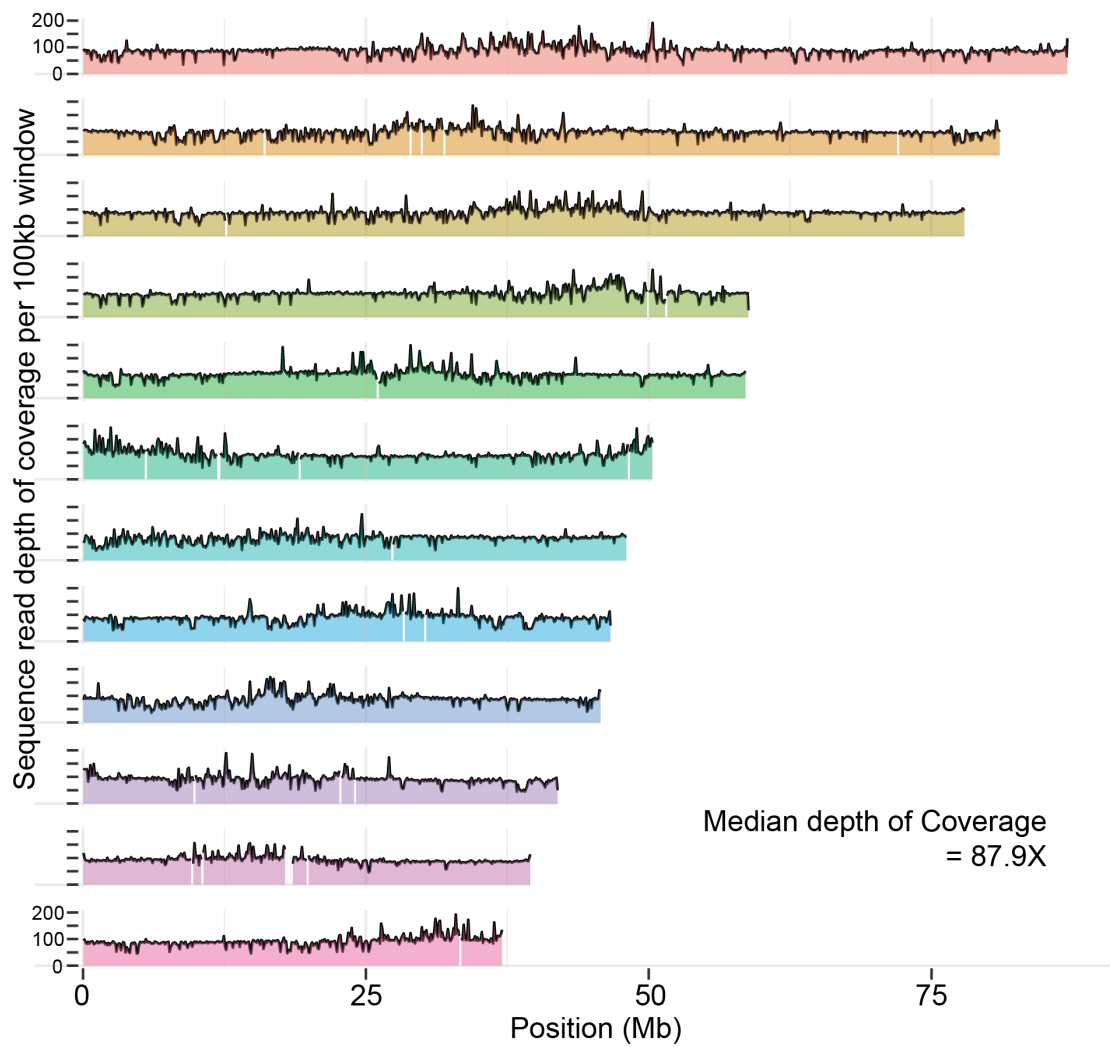
Supplementary Fig. 2. Estimate of genome size from Illumina paired end sequences of SCT using Genomescope³.



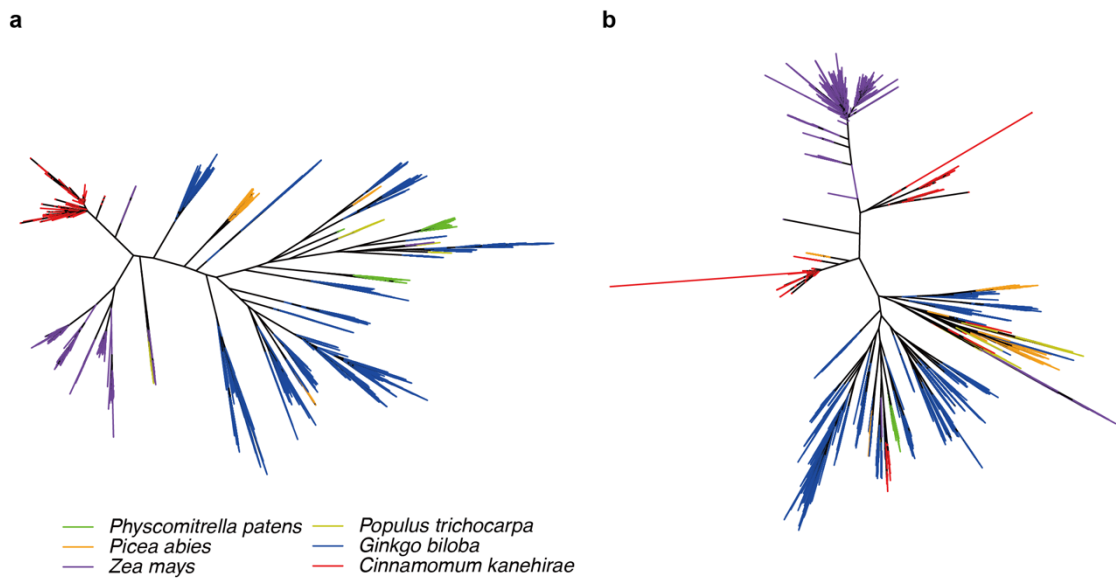
Supplementary Fig. 3. Contact matrices of the largest 12 scaffolds of the final SCT assembly. Hi-C reads were realigned back to the assembly and the mappings were converted to the dot intensity which indicate the likelihood of loci collocate in the nucleus.



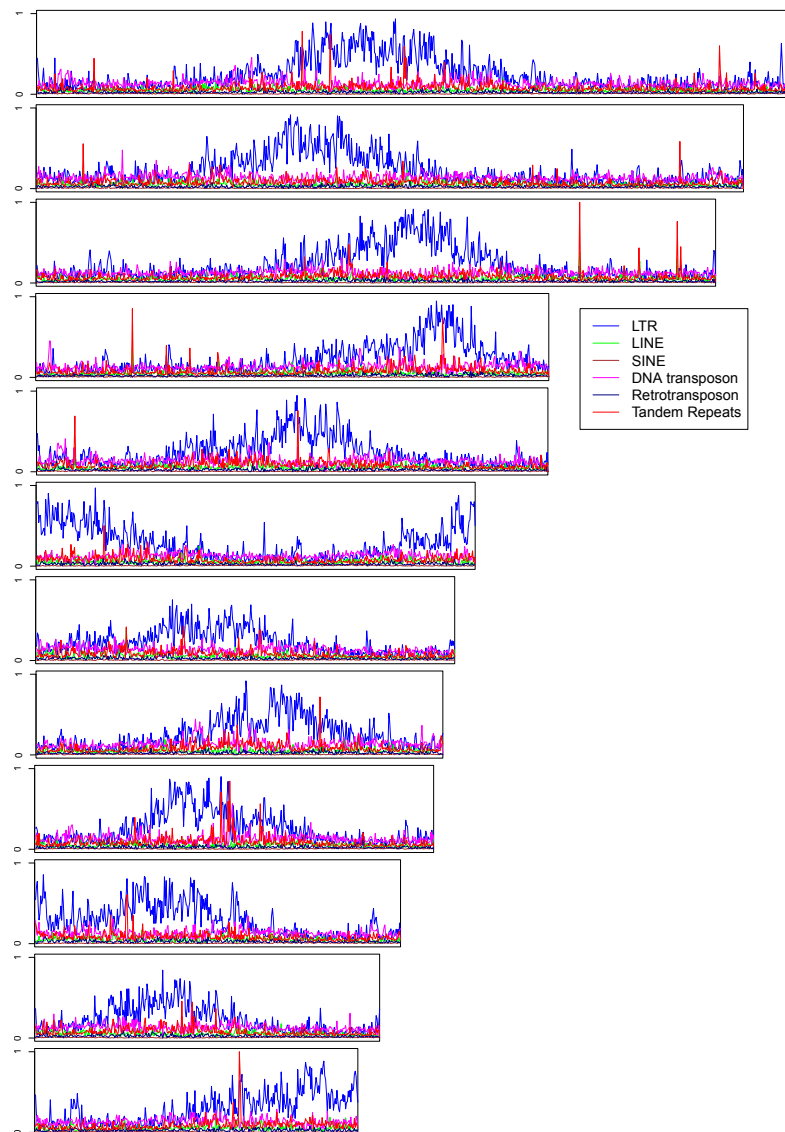
Supplementary Fig. 4. Distribution of alternative (non-reference) allele frequency on the largest 12 scaffolds of SCT. One density is shown for each scaffold.



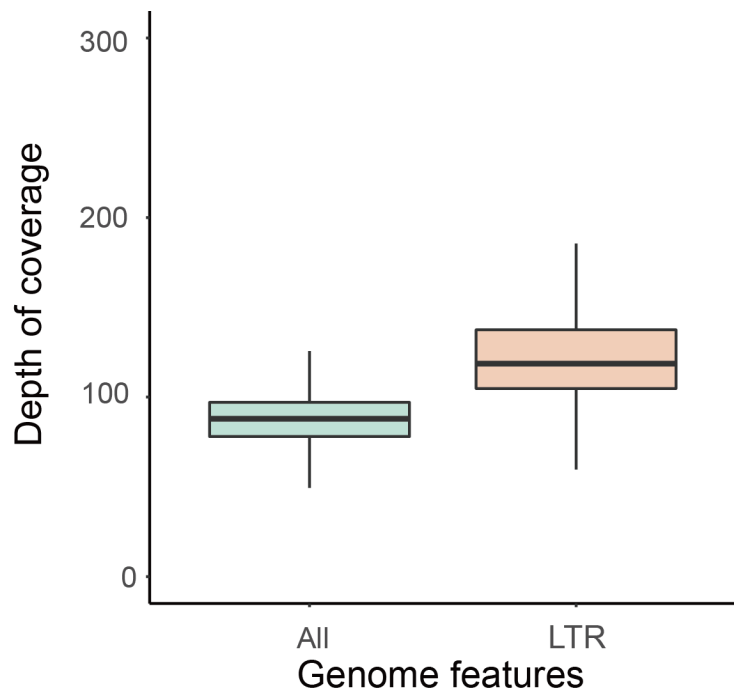
Supplementary Fig. 5. Sequence Mapping profile in SCT. Depth of Illumina genomic DNA sequencing coverage along the non-overlapping 100 kb windows of largest 12 scaffolds of SCT.



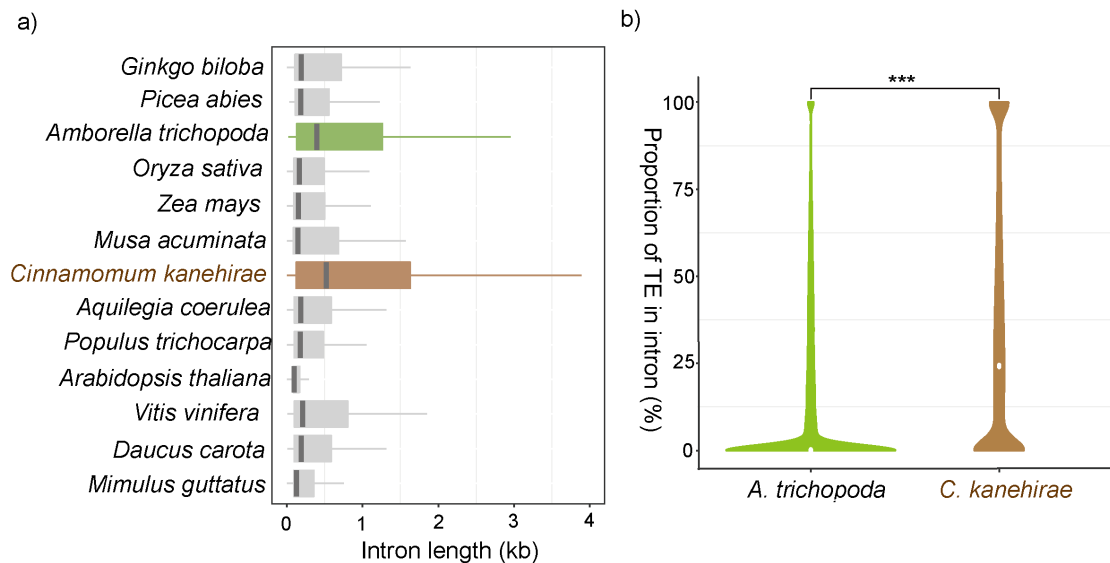
Supplementary Fig. 6. Phylogenetic relationships of LTR-RT domains. **a**, Inferred from Ty3/Gypsy. **b**, Inferred from Ty1/Copia LTR-RT domains. Branches are color-coded according to species.



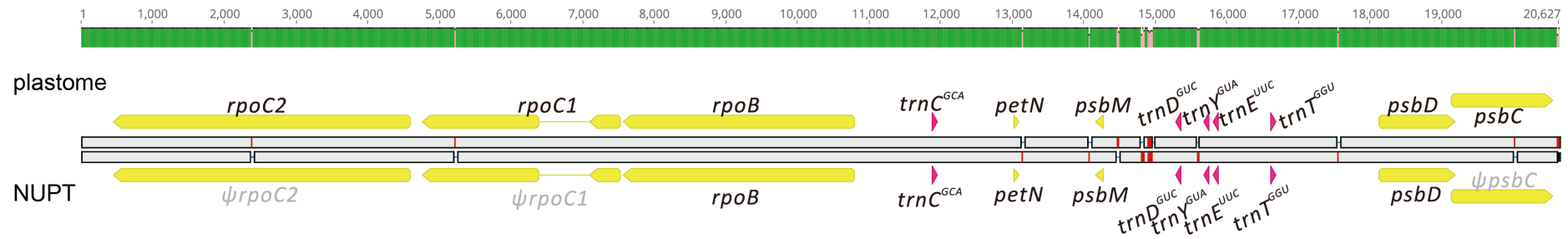
Supplementary Fig. 7. Distribution of TEs and genes along the 12 largest scaffolds of SCT.



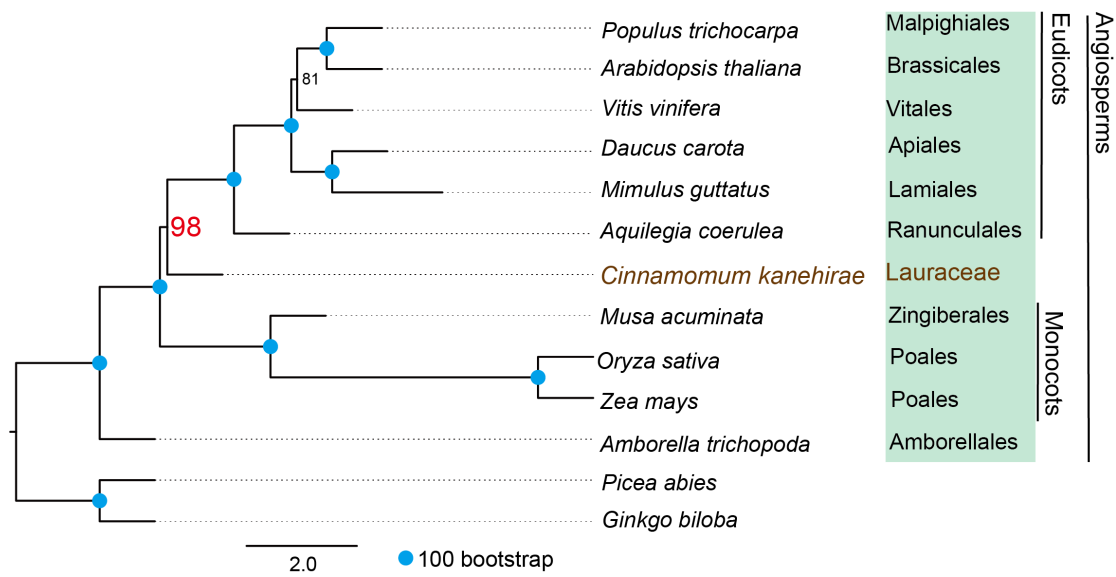
Supplementary Fig. 8. Boxplot of depth of coverage in LTR enriched windows (n= 249, Minium = 32.7X , Maximum = 236.1X, Median = 118.6X, 1st Quartile = 104.8X, 3rd Quartile = 137.4X,)versus all windows (n= 9,013, Min. = 0.08X , Max. = 15,042.3X, Median = 87.9X, 1st Qu. = 78.0X, 3rd Qu. = 97.0X)in the genome. The LTR enriched genome windows have a median of 118.6X, which is 35% higher.



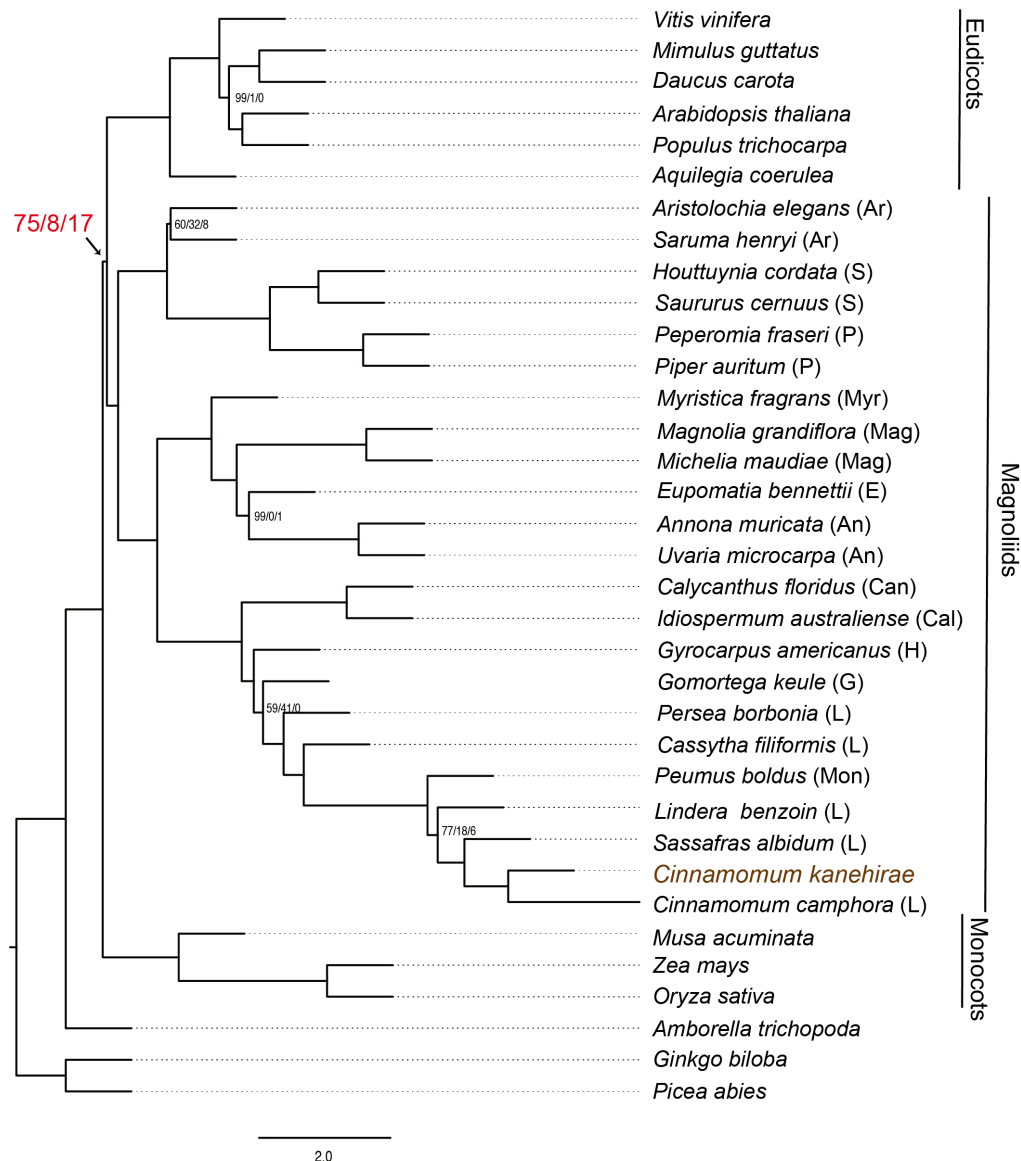
Supplementary Fig. 9. Intron dynamics of SCT. **a,** Distribution of intron length across plants (*Mimulus guttatus*, n = 117,749, Minimum = 3.0, 1st Quartile = 94.0, Median = 128.0, 3rd Quartile = 356.0, Maximum = 8135.0; *Daucus carota*, n = 128,674, Min. = 10.0, 1st Qu. = 97.0, Median = 193.0, 3rd Qu. = 584.0, Max. = 41367.0; *Vitis vinifera*, n = 135,706, Min. = 8.0, 1st Qu. = 102.0, Median = 211.0, 3rd Qu. = 802.0, Max. = 39915.0; *Arabidopsis thaliana*, n = 118,640, Min. = 1.0, 1st Qu. = 85.0, Median = 99.0, 3rd Qu. = 167.0, Max. = 11601.0; *Populus tricocarpa*, n = 166,138, Min. = 1.0, 1st Qu. = 100.0, Median = 178.0, 3rd Qu. = 480.0, Max. = 10052.0; *Aquilegia coerulea*, n = 121,035, Min. = 1.0, 1st Qu. = 99.0, Median = 181.0, 3rd Qu. = 584.0, Max. = 10990.0; *Cinnamomum kanehirae*, n = 122,991, Min. = 2, 1st Qu. = 122, Median = 524, 3rd Qu. = 1629, Max. = 239861; *Musa acuminata*, n = 163,062, Min. = 1.0, 1st Qu. = 88.0, Median = 148.0, 3rd Qu. = 680.0, Max. = 25265.0; *Zea mays*, n = 167,171, Min. = 1.0, 1st Qu. = 93.0, Median = 155.0, 3rd Qu. = 500.0, Max. = 169079.0; *Oryza sativa*, n = 145,228, Min. = 4.0, 1st Qu. = 94.0, Median = 163.0, 3rd Qu. = 491.0, Max. = 18326.0; *Amborella trichopoda*, n = 82,937, Min. = 20, 1st Qu. = 134, Median = 394, 3rd Qu. = 1263, Max. = 175747; *Picea abies*, n = 107,313, Min. = 33.0, 1st Qu. = 112.0, Median = 182.0, 3rd Qu. = 558.0, Max. = 68268.0; *Ginkgo biloba*, n = 135,813, Min. = 1, 1st Qu. = 109, Median = 190, 3rd Qu. = 719, Max. = 1272917). **b,** Wilcoxon-rank sum test shows that the distribution of TE proportion in intron is significantly different (P = 4.79e-181; two-sided Wilcoxon rank sum test) between *C. kanehirae* and *A. trichopoda*. (*C. kanehirae*, n = 122,991, Min. = 0.00, 1st Qu. = 0.00, Median = 24.22, 3rd Qu. = 58.44, Max. = 100; *A. trichopoda*, n = 82,937, Min. = 0.00, 1st Qu. = 0.00, Median = 0.00, 3rd Qu. = 22.73, Max. = 100)



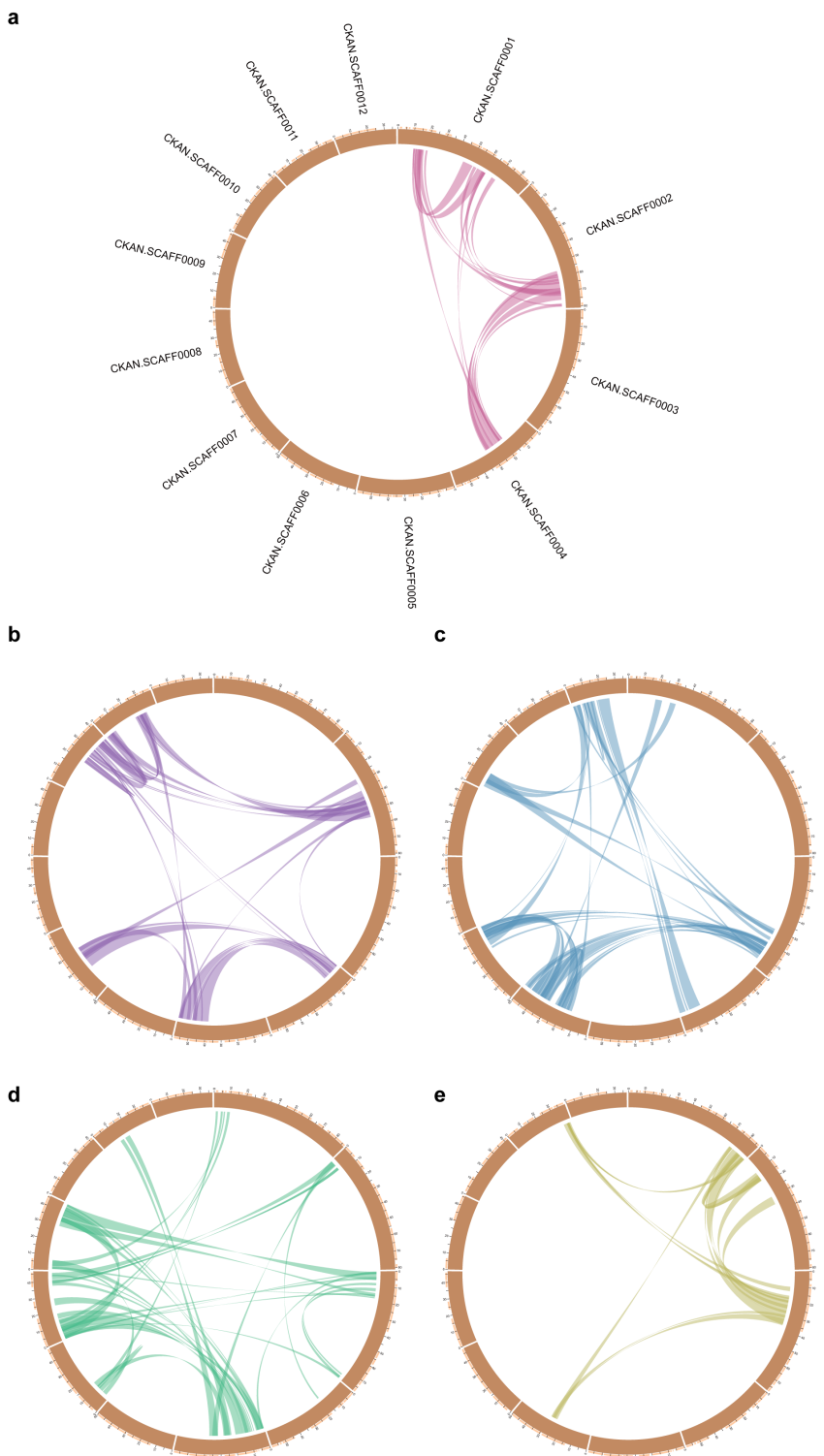
Supplementary Fig. 10. Sequence alignment of the longest NUPT found in SCT genome to its counterpart in plastome. The histograms represent sequence similarity colored as green (100%) and light pink (< 100%). Protein-coding and tRNA genes were denoted as yellow and pink arrows, respectively. Red and blue lines in the alignment indicate nucleotide differences and gaps between the two sequences. Pseudogenes were marked with psi (Ψ) symbol and labeled in gray fonts. Three out of the seven protein-coding genes were pseudogenized.



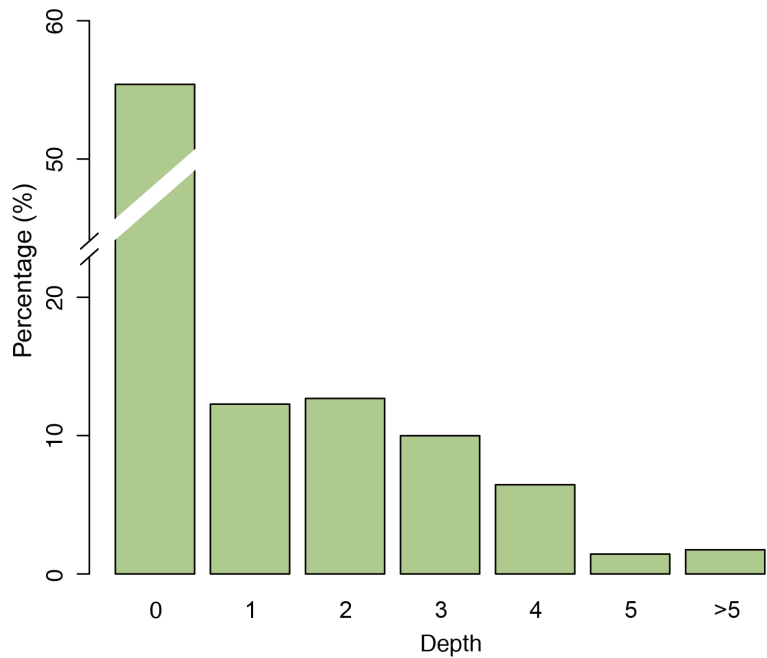
Supplementary Fig. 11. A species tree of 13 plant species based on the coalescence of gene trees constructed from protein sequence alignment of each of 211 single-copy orthologues using ASTRAL⁴. Number or blue dots on every node represent the proportion of gene trees that support each node.



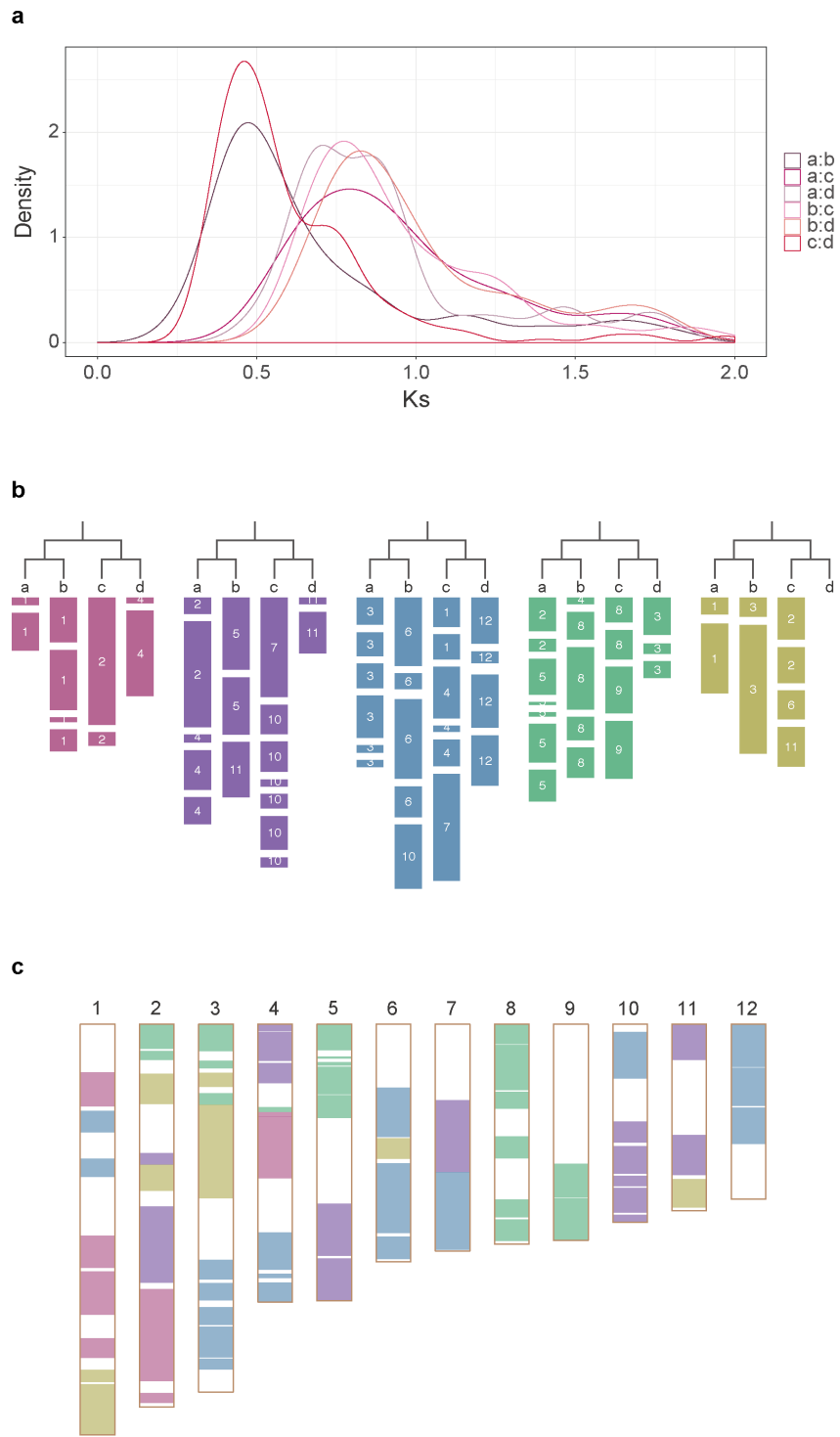
Supplementary Fig. 12. A species tree of 35 plant species based on the coalescence of gene trees using ASTRAL⁴. Gene trees were constructed from protein sequence alignment of each of 211 orthogroups inferred previously with the dataset of 13 species using RAxML⁶ with 100 bootstrap replicates (options: -m PROTGAMMAILGF -f a). In each orthogroup, missing data were tolerated or one gene chosen from random for each of the additional species from 1KP⁵. Number on every node represent the local posterior probabilities of main topology and two alternatives. All nodes have 100/0/0 local posterior support unless stated otherwise. Bracket next species' name denote different families: Ar, Aristolochiaceae; S, Saururaceae; P, Piperaceae; Mon, Monimiaceae; Myr, Myristicaceae; Mag, Magnoliaceae; E, Eupomatiaceae; An, Annonaceae; Can, Canellaceae; Cal, Calycanthaceae; H, Hernandiaceae; G, Gomortegaceae; L, Lauraceae.



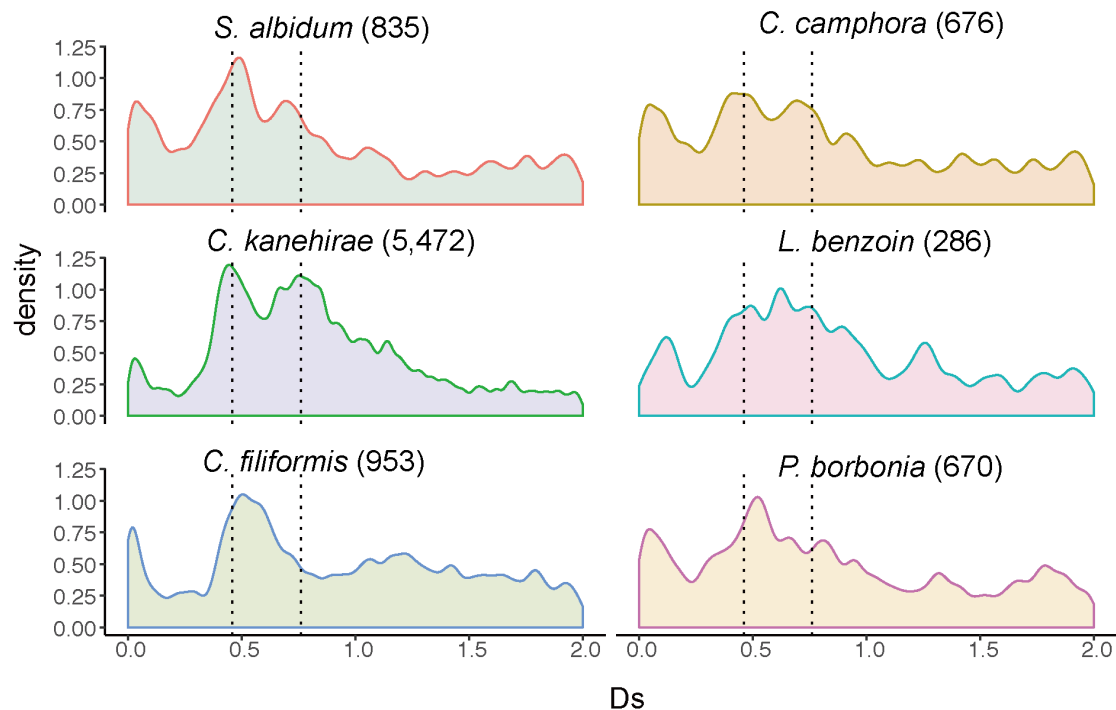
Supplementary Fig. 13. Assignment of synteny blocks into five linkage clusters.



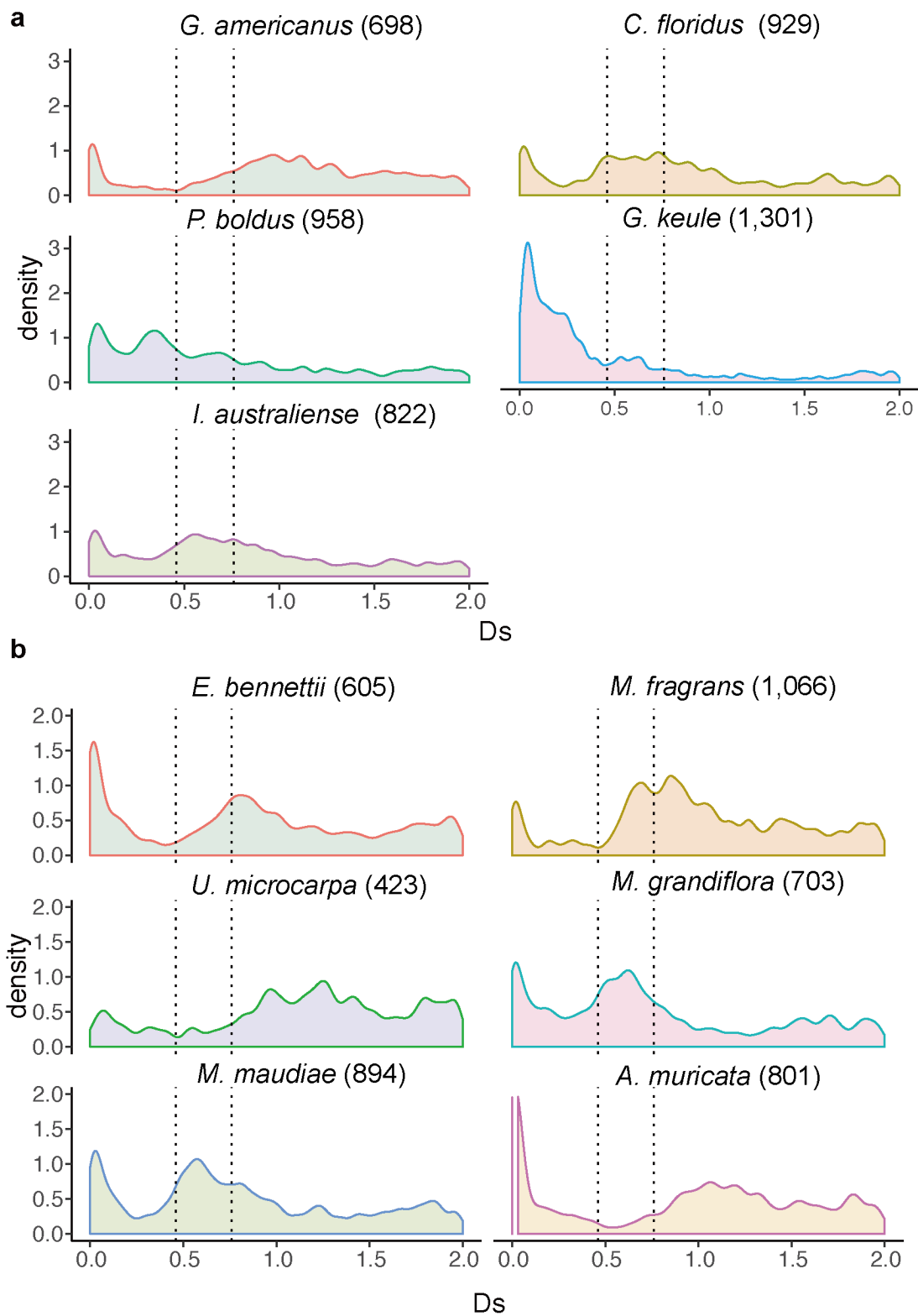
Supplementary Fig. 14. Observed depth of syntentic block coverage in the genome of SCT for every syntetic region of *A. trichopoda*. For example, 6.5% of *A. trichopoda* genome can be found in syntetic in four regions of SCT.



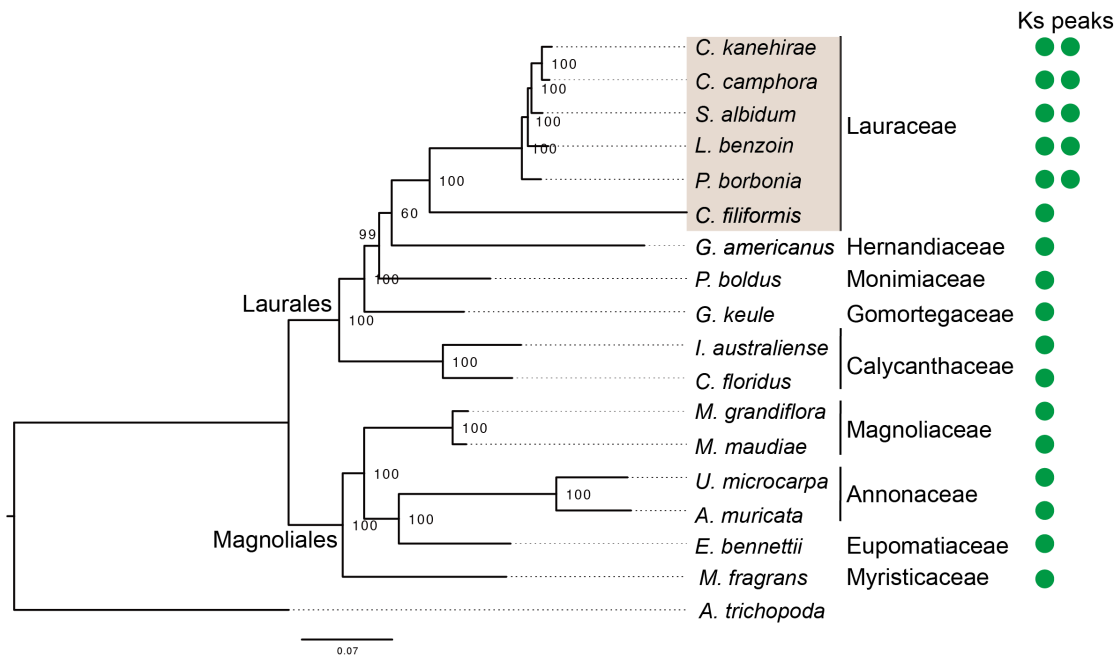
Supplementary Fig. 15. Infragenomic synteny block assignment and proposed karyotype evolution in SCT. **a**, Chromosomes in pairs that arose after each WGD events were identified based on whether Ks distribution was peaked at ~ 0.46 (second WGD) or ~ 0.76 (first WGD). **b**, Proposed karyotype type of the synteny blocks **c**. Different color representing one of the five ancestral chromosomes plotted on the twelve SCT chromosomes.



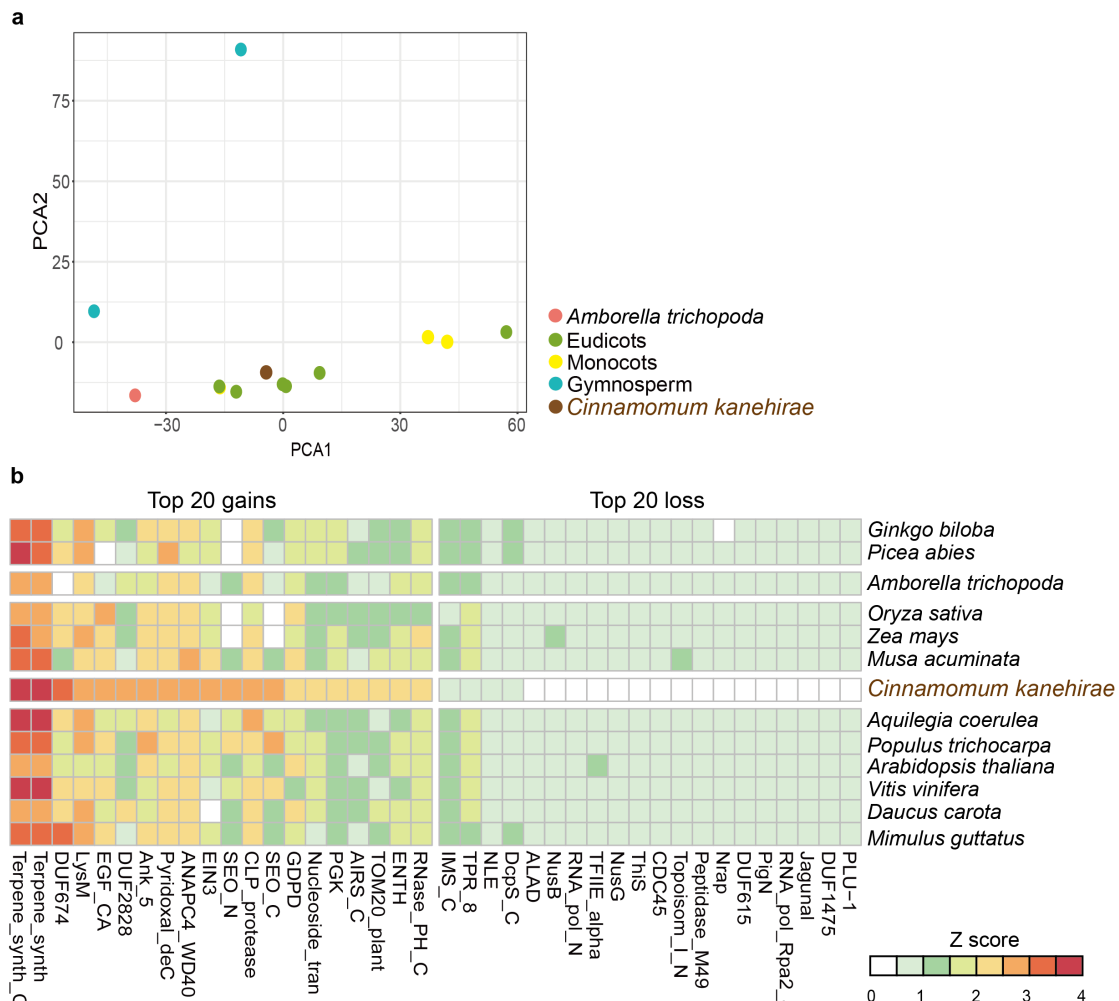
Supplementary Fig. 16. Density plots of synonymous substitutions (Ks) of Lauraceae in the 1KP⁵ and SCT. Dashed lines denote the two Ks peaks observed in SCT. Number in brackets denote number of available pairwise intragenomic orthologues in each species.



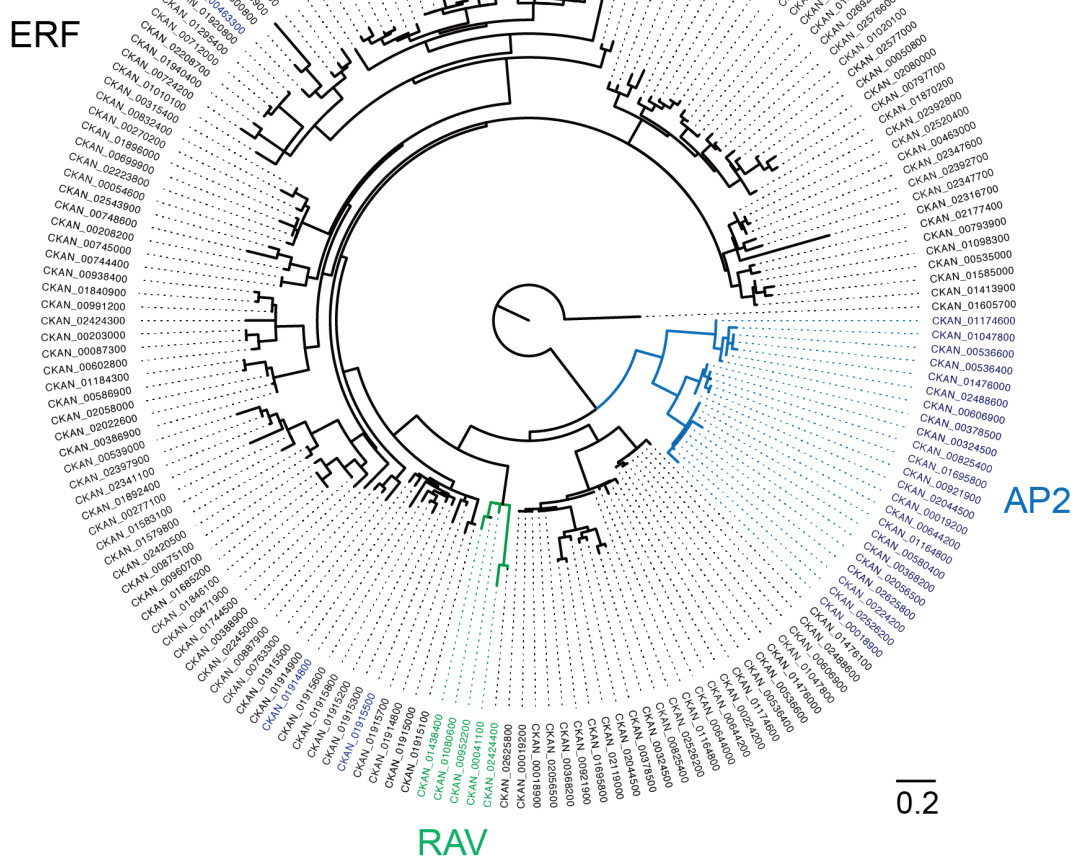
Supplementary Fig. 17. Density plots of synonymous substitutions (Ks) of intragenomic pairwise duplicates of **a, Laurales outside Lauraceae. **b**, Magnoliales in the 1KP⁵. Dashed lines denote the two Ks peaks observed in SCT. Number in brackets denote number of available pairwise intragenomic orthologues in each species.**



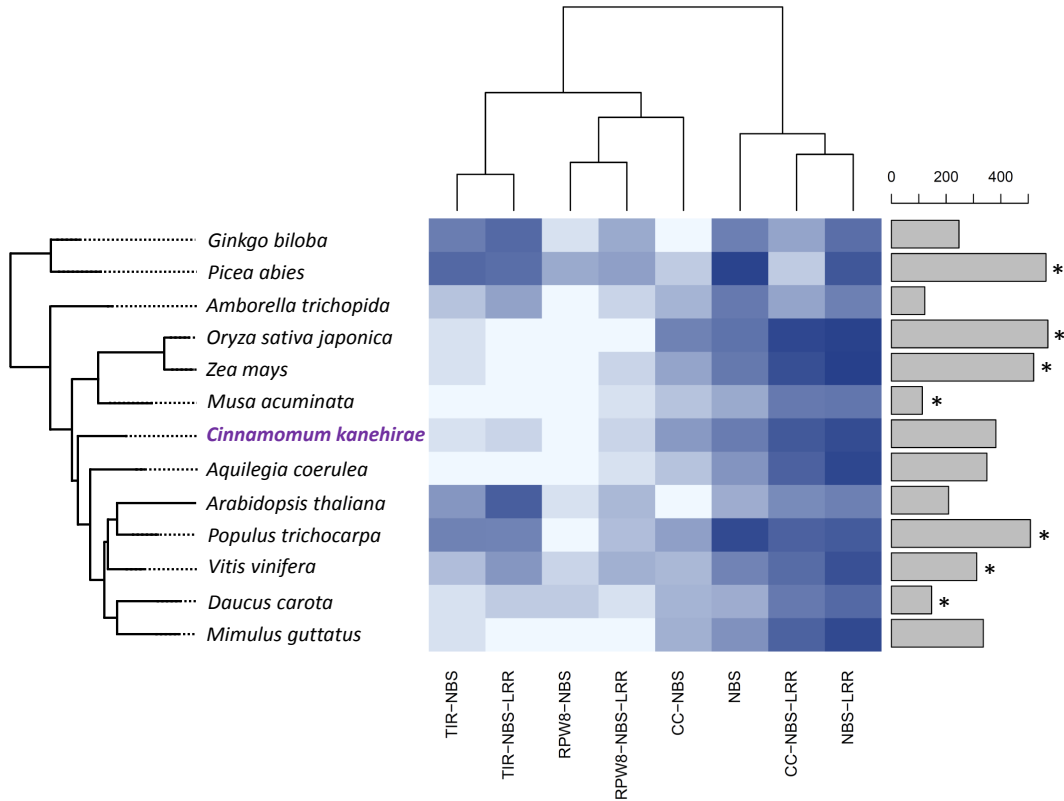
Supplementary Fig. 18. Phylogenomic analysis of Lauraceae WGD events. The two identified WGD events are placed on the phylogeny as circles. The tree shows the relationship of *C. kanehirae*, Laurales and Magnoliales from 1KP⁵. The maximum likelihood phylogeny was produced using concatenated amino acid alignment of 69 single copy orthologs using RAxML⁶ with 500 bootstrap replicates (options: -m PROTGAMMAILGF -f a).



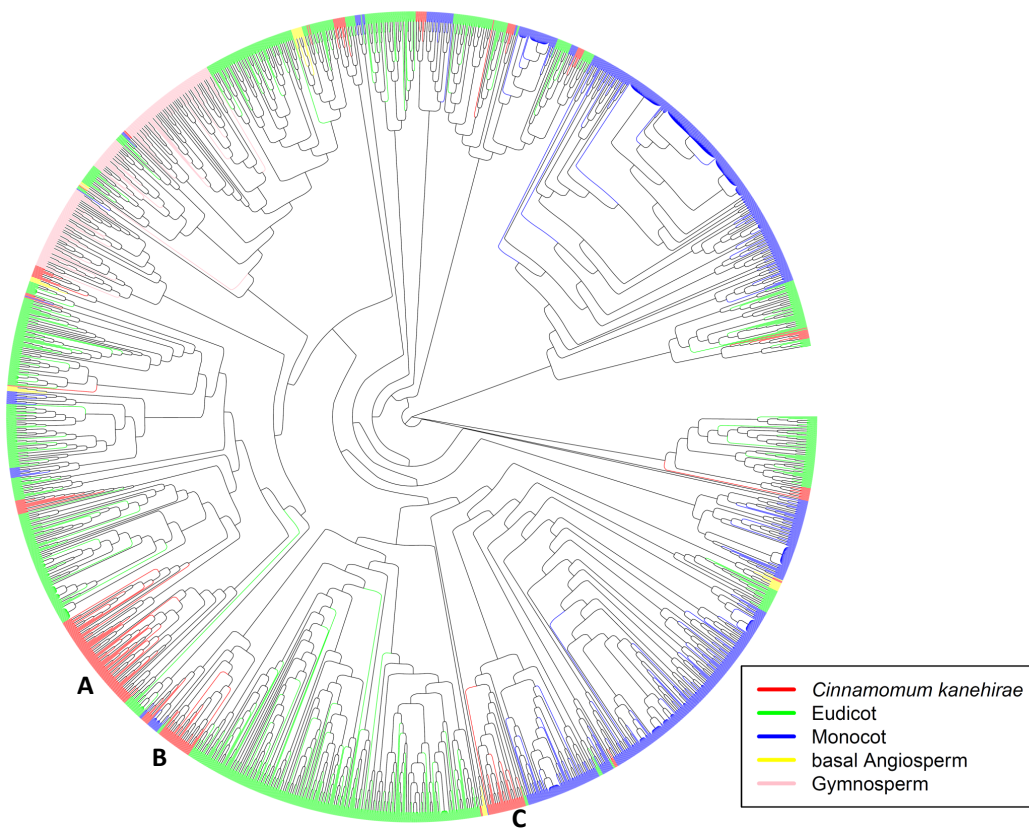
Supplementary Fig. 19. Protein family domain (Pfam) analysis across 13 plant species. **a**, Principal component analysis of numbers in 4,455 Pfams. **b**, Top 20 enrichment of Pfam gains and loss in *C. kanehirae* sorted by domain counts. For every Pfam a z-score was calculated for the corresponding abundance in each species. Only z-scores greater than 1.96 and -1.96 were included and shown in Supplementary Table 9.



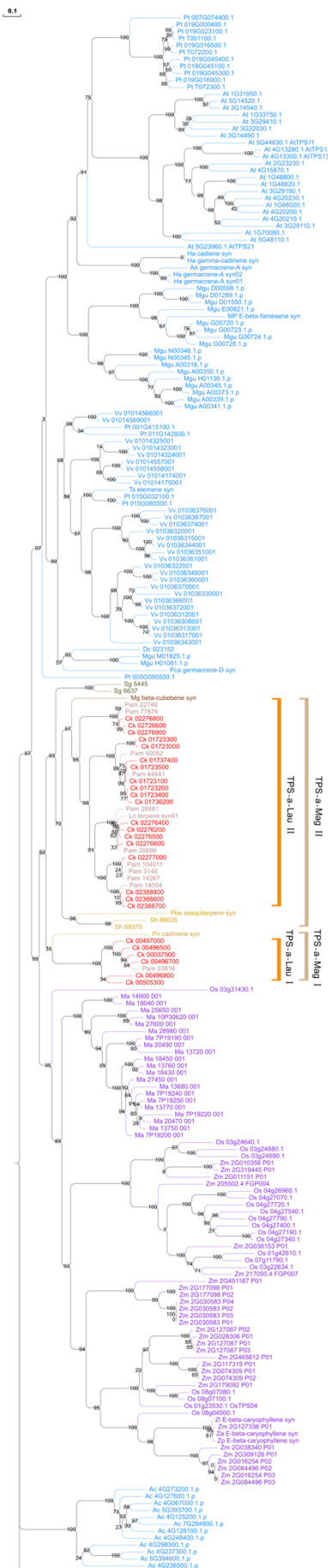
Supplementary Fig. 20. Phylogeny of APETALA2/Ethylene-responsive element binding protein (AP2/EREBP)-type transcription factors. The maximum likelihood phylogeny was constructed from alignment of the AP2 (PF00847) domain of proteins using RAxML⁶. The AP2/EREBP members were classified according to their phylogenetic positions and domain combination: AP2 with two AP2 domains (23 members); RAV (related to ABI3/VP) with a single AP2 and an additional B3 domain (four members), and rest being ethylene response factors (ERF; 150 members).



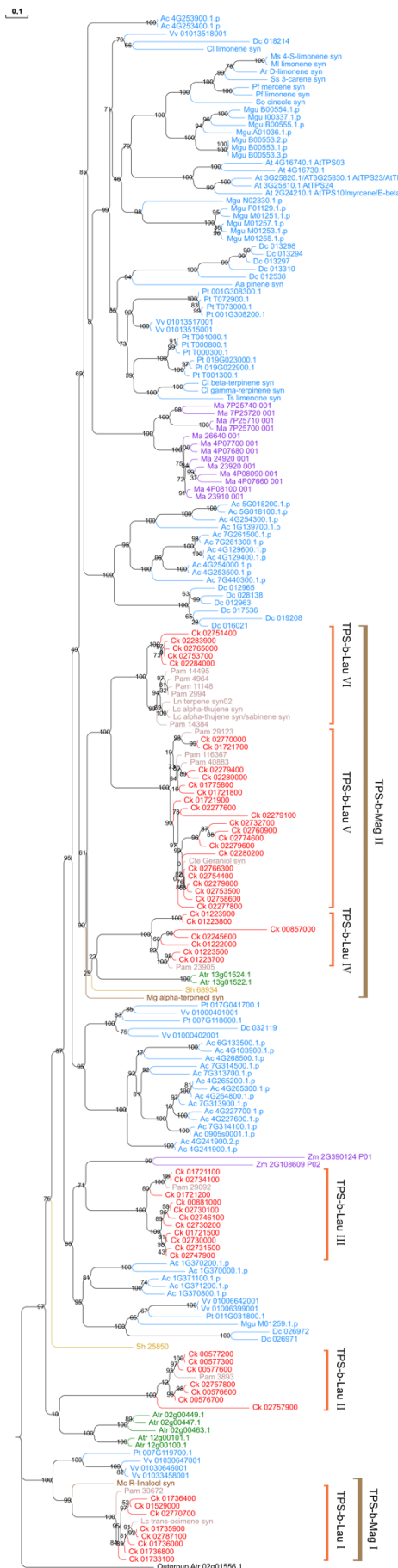
Supplementary Fig. 21. The distribution of resistance genes in the 13 species. The phylogenetic tree on the left side was derived from the tree built from 211 single copy genes. Darker and lighter colors in the heatmap indicate higher and lower numbers of corresponding resistance gene types, respectively. The hierarchical clustering tree at the top indicates the clustering of different resistance gene types across the species. The bar chart on the right side represents the total number of resistance genes for the 13 species. Asterisks (*) denote cultivated species.



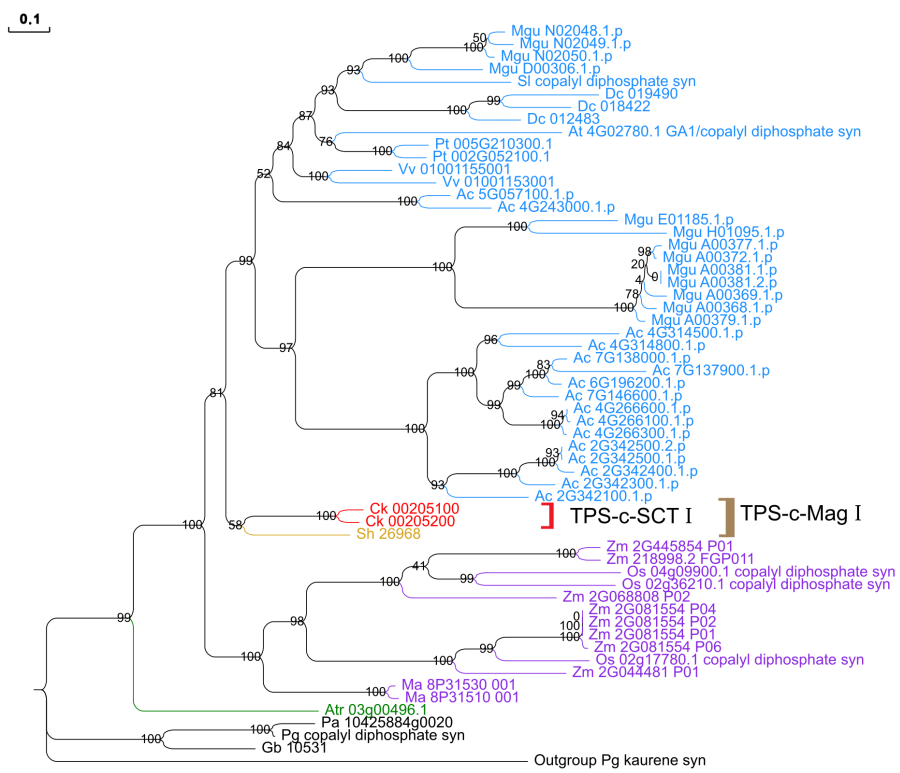
Supplementary Fig. 22. The phylogenetic tree of the NBS domain of the resistance genes. The three bold letters indicate major branching events of NBS domains in the resistance genes occurred in the evolutionary history of *C. kanehirae*.



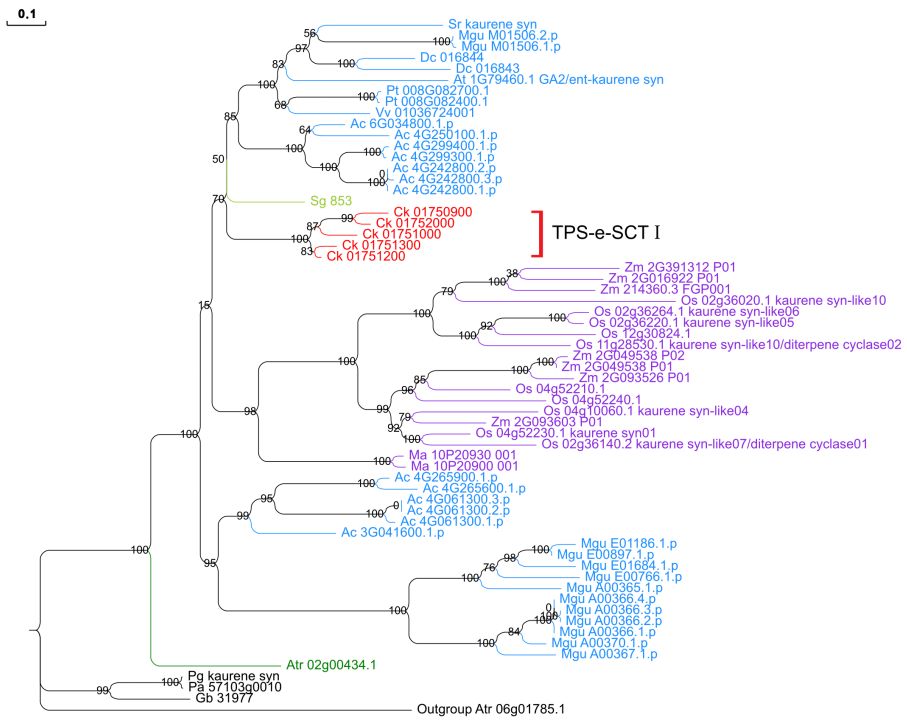
Supplementary Fig. 23. Phylogeny of the TPS-a subfamily from available magnoliids and the 13 sampled taxa. An *Amborella* TPS gene of TPS-g is chosen as the outgroup. The TPS-a subfamily of available magnoliids (including Piperales, Magnoliales, and Lauraceae) and Chloranthales (*Sarcandra*) formed a monophyletic clade with the TPS of monocots. Within the magnoliids, there are two well supported subclades—TPS-a-Mag I and TPS-a-Mag II—and one unresolved subclade containing only the cadinene synthase in *Piper nigrum*. The Lauraceae TPS genes form two monophyletic clades. The six members of TPS-a-Lau I are close to the cadinene synthase in *Piper nigrum*. The other 19 CkTPS-a formed four subgroups, each containing at least two TPS from *Persea* and one also containing TPS from *Laurus nobilis*. These four subclade are sister to the -cubene synthase in *Magnolia grandiflora* with 97% bootstraps support. The tree topology and placements of Lauraceous TPS data suggest that the TPS-a subfamily has duplicated at least five times in Lauraceae and 10 times within SCT. The 25 CkTPSs of TPS-a encode at least three kind of different TPSs. Aa, *Artemisia annua*; Ac, *Aquilegia coerulea*; Ag, *Abies grandis*; Am, *Antirrhinum majus*; Ar, *Agastache rugosa*; At, *Arabidopsis thaliana*; Atr, *Amborella trichopoda*; Cc, *C. camphora*; Ck, *C. kanehirae*; Cl, *Citrus limon*; Ct, *Cycas taitungensis*; Cte *C. tenuipile*; Cm, *C. micranthum*; Co, *C. osmophleum*; Es, *Ephedra sinica*; Gb, *Ginkgo biloba*; Ha, *Helianthus annuus*; Lc, *Litsea cubeba*; Ln, *Laurus nobilis*; Mc, *Magnolia champaca*; Mg, *M. grandiflora*; Mgu, *Mimulus guttatus*; Ml, *Mentha longifolia*; MP, *Mentha x Piperita*; Ms, *Mentha spicata*; Os, *Oryza sativa*; Pa, *Picea abies*; Pam, *Persea americana*; Pb, *Pinus banksiana*; Pbe, *Piper betle*; Pc, *Pogostemon cablin*; Pf, *Perilla frutescens*; Pg, *Picea glauca*; Pn, *Piper nigrum*; Sh, *Saruma henryi*; Sl, *Solanum lycopersicum*; So, *Salvia officinalis*; Sr, *Stevia rebaudiana*; Ss, *S. stenophylla*; Ts, *Toona sinensis*; Vv, *Vitis vinifera*; Za, *Zea mays*; Zl, *Z. luxurians*; Zp, *Z. perennis*.



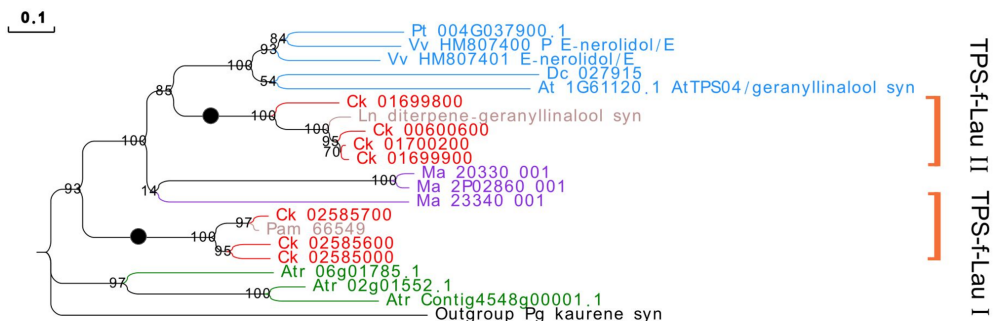
Supplementary Fig. 24. Phylogeny of the TPS-b subfamily from available magnoliids and the 13 sampled taxa. An *Amborella* TPS-g sequence is chosen as the outgroup (the same as in the TPS-a). Two monophyletic magnoliids-TPS-b are resolved. A total of 58 CkTPSs form at least six Lauraceae subgroups in TPS-b. In detail, TPS-b-Lau I was clustered with a R-linalool synthase from *Magnolia champaca*, which is shown as TPS-b-Mag I in the figure, and it clusters with the eudicot-specific subgroup with 100% bootstrap support. TPS-b-Lau II contains seven CkTPSs and one PaTPS, and five *Amborella* TPSs but with only 10% bootstrap values. TPS-b-Lau III, two maize TPSs, and a well-supported eudicot clade (containing eleven TPSs) together form a highly supported cluster (95% bootstrap replicates). TPS-b-Mag II is divided into three subgroups: TPS-b-Lau IV, TPS-b-Lau V, and TPS-b-Lau VI. This tree topology suggests that 32 paralogous duplication events have occurred in CkTPS genes.



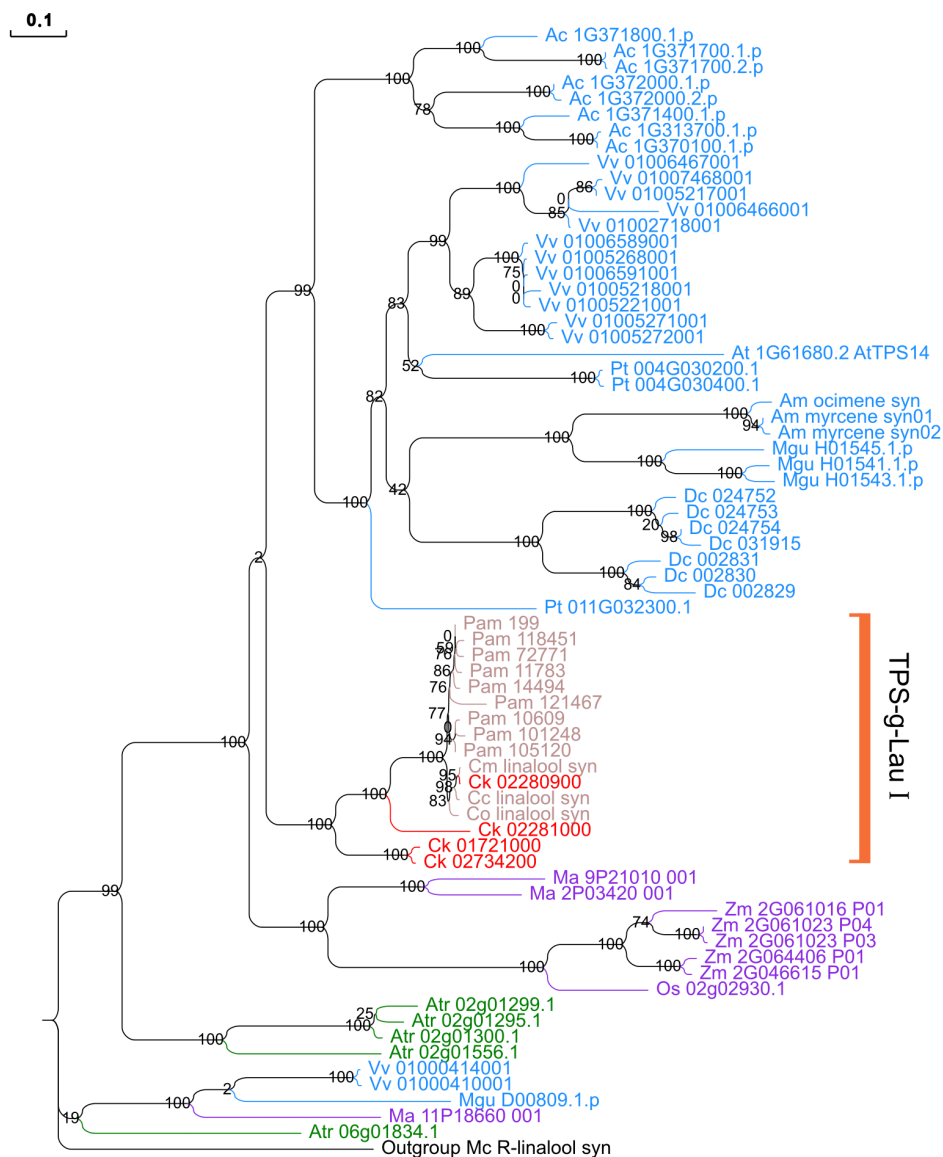
Supplementary Fig. 25. Phylogeny of the TPS-c subfamily from available magnoliids and the 13 sampled taxa. A kaurene synthase gene in *Picea glauca* from the TPS-e subfamily is chosen as the outgroup. Two CkTPSs and one *Saruma* TPS are clustered together in one clade, labeled “TPS-c-Mag I” in the figure. In subfamily TPS-c, the magnoliids-clade is clustered with eudicots. This tree topology suggests that there is only one paralogous duplication.



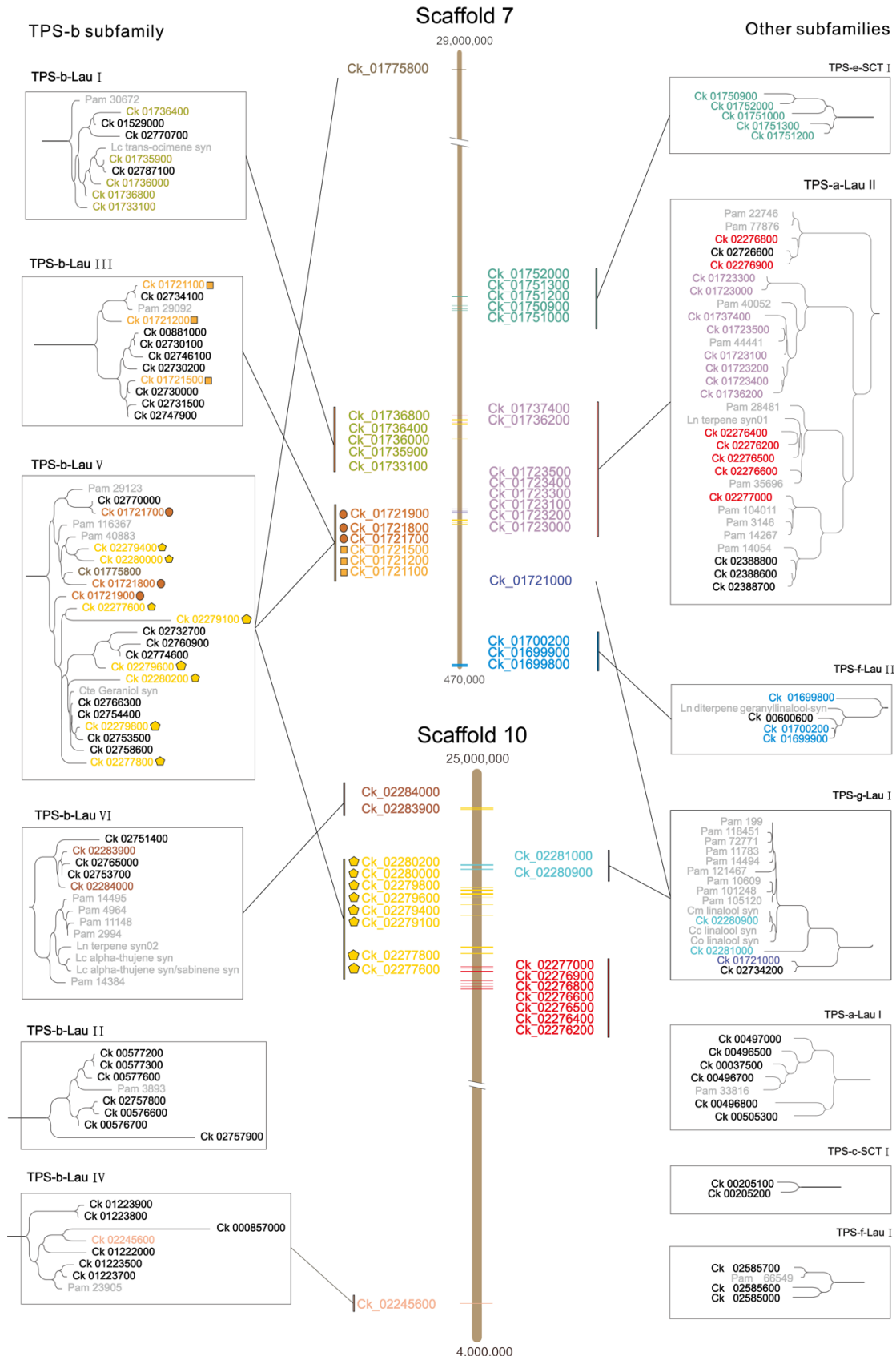
Supplementary Fig. 26. Phylogeny of the TPS-e subfamily from available magnoliids and the 13 sampled taxa. An *Amborella* TPS of TPS-f was chosen as the outgroup. All sampled eudicots form three monophyletic clades, and the TPSs of all three monocots form a monophyletic group. The five CkTPSs also form a monophyletic clade, TPS-e-SCT I, which is sister to one *Sarcandra* TPS and a group of eudicot-specific TPS but with low bootstrap supports (70%). The TPS-e-SCT I likely had four paralogous duplications based on this tree topology.



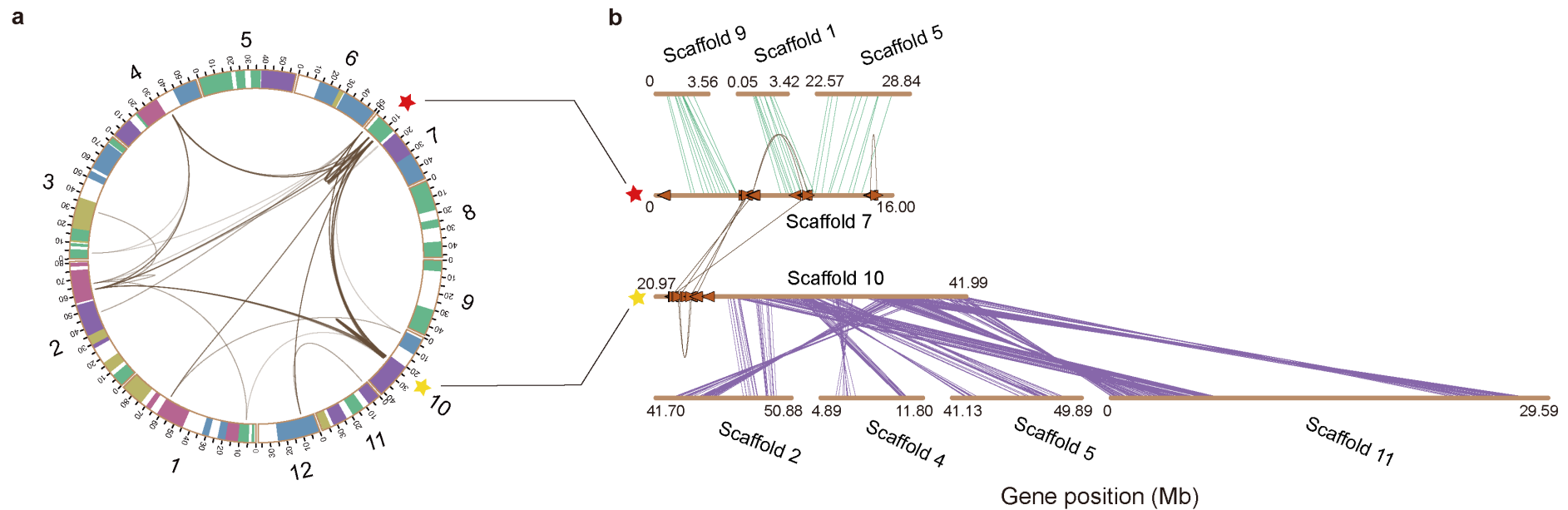
Supplementary Fig. 27. Phylogenetic analysis of the TPS-f subfamily from all available magnoliids and the 13 sampled taxa. As TPS-f subfamily genes were not found in gymnosperms, a kaurene synthase gene in *Picea glauca* from the subfamily TPS-e was chosen as the outgroup. Two Lauraceae-specific groups, TPSf-Lau I and TPS-f-Lau II, are resolved. TPS-f-Lau I is sister to a large clade containing three banana TPSs, TPS-f-Lau II, and a eudicots clade consisting of five TPSs, and the latter two form a well-supported monophyletic group (85%). The four CkTPS genes in TPS-f-Lau II likely code for the geranyl linalool synthase as they are clustered with the geranyl linalool synthase gene of *Laurus nobilis*. This tree topology suggests that there are a total of three CkTPS-specific duplication events. The branches labeled with circles were used to detect positive selection under the branch-site model analysis (Supplementary Table 13).



Supplementary Fig. 28. Phylogeny of the TPS-g subfamily from all available magnoliids and the 13 sampled taxa. As gymnosperms do not have TPS-g subfamily genes, a R-linalool synthase in *Magnolia champaca* from TPS-b was chosen as the outgroup. The TPS-g-Lau I is resolved as a monophyletic clade and subdivided into three subclades, one *PaTPs*-specific group, one *Cinnamomum*-specific group (all linalool synthase), and two CkTPS groups. However, the relationships among TPS-g-Lau I, monocots, and eudicots are not resolved. This tree topology suggests that there is only one CkTPS-specific duplication (paralogous).



Supplementary Fig. 29. Chromosome localization of CkTPS genes on scaffolds 7 and 10. The horizontal bars coded with colors correspond to TPS gene subfamilies in Supplementary Table 12. Phylogenetic trees within boxes (at the both sides of the scaffolds) correspond to Lauraceae-specific or SCT-specific subclades in the trees of each TPS subfamily (Supplementary Fig. 23–28). Genes on each partial tree in boxes are connected by lines to their locations in scaffolds. For visualization purposes, genes from the same sub-family were labeled in same color and icons (circle, square, and pentagon). CkTPS genes that located at other scaffolds and non-CkTPS genes were labeled in black and gray, respectively.



Supplementary Fig. 30. Chromosome localization of CkTPS genes on the largest 12 scaffolds. a, A circos plot showing distribution of CkTPS with links denoting CkTPS of different subfamilies. Numbers denote different scaffolds. Clustering of CkTPS on scaffold 7 and 10 were apparent. **b,** Schematic representation of intragenomic relationship amongst the synteny blocks around the CkTPS gene clusters. Lines denote orthologs defined by DAGchainer¹ and different colors denote assigned linkage groups.

III. SUPPLEMENTARY TABLES

Supplementary Table 1. Genome summary of *C. kanehirae* and 12 other plant species.

	<i>A. trichopoda</i>	<i>A. coerulea</i>	<i>A. thaliana</i>	<i>C. kanehirae</i>	<i>D. carota</i>	<i>G. biloba</i>	<i>M. acuminata</i>	<i>M. guttatus</i>	<i>O. sativa</i>
Genome size (Mb)	706.3	306.5	119.7	730.7	421.5	10,608.7	473.0	312.7	374.5
Scaffold number (n)	5,745	1,034	7	2,153	4,826	12	12	1,507	14
N50 (Mb)	4.9	43.6	23.5	50.4	36.6	1.4	34.1	21.2	30.0
Number of genes	27,313	30,023	27,416	27,899	32,113	36,528	36,528	28,140	42,189
Gene length (Mb)	153.1	107.5	60.5	235.6	100.1	1,122.5	138.9	77.1	121.1
Exon number	110,895	139,263	140,303	150,741	160,787	197,588	197,588	139,382	177,615
Exon length (Mb)	25.7	33.9	33.1	36.4	38.0	49.5	37.7	33.3	46.6
Intron length (Mb)	127.4	73.6	27.3	199.2	62.1	1,073.0	101.2	43.8	74.5
Intergene length (Mb)	553.2	199.1	59.2	494.8	321.4	9,486.2	334.0	235.7	253.4
BUSCO (%)	85.2	95.8	99.3	88.5	83.2	62.8	86.7	94.5	95.6

	<i>P. abies</i>	<i>P. trichocarpa</i>	<i>V. vinifera</i>	<i>Z. mays</i>
Genome size (Mb)	12,301.4	473.2	434.1	2,067.9
Scaffold number (n)	10,253,694	1,446	33	523
N50 (Mb)	0.0	17.4	19.5	23.0
Number of genes	70,736	41,335	26,346	63,480
Gene length (Mb)	171.7	107.7	128.4	170.0
Exon number	178,049	196,772	156,765	224,101
Exon length (Mb)	51.1	36.8	47.1	29.8
Intron length (Mb)	120.6	70.9	81.4	140.2
Intergene length (Mb)	12,129.6	365.6	305.7	1,897.9
BUSCO (%)	38.6	97.6	90.0	92.2

Supplementary Table 2. Summary of transcriptome dataset

Sample origin	Stage type ¹	Read length (bp)	Library size (bp)	num. reads	Accession
Flower buds	1	90	4,933,823,400	54,820,260	SRR7416917
Immature leaf	2	90	5,090,668,920	56,562,988	SRR7416906
Flower buds	3	90	5,395,165,920	59,946,288	SRR7416909
Old leaf	4	90	5313249000	59,036,100	SRR7416908
Young leaf	5	90	3,084,625,440	34,273,616	SRR7416918
Young stem	6	90	4,511,830,680	50,131,452	SRR7416905
Flowers	7	90	4,764,666,420	52,940,738	SRR7416910
Fruits	8	90	4,356,926,640	48,410,296	SRR7416911

¹Photos of the stages are given in Supplementary Fig. 1c.

Supplementary Table 3. Statistics of orthologous group (OG) inferred by Orthofinder

Supplementary Table 3 is an Excel file.

Supplementary Table 4. Enriched gene ontology (GO) terms of genes located in region of heterozygosity (ROH)

Supplementary Table 4 is an Excel file.

Supplementary Table 5. Repeat content

Repeat classes	Genome proportion
LINE	5.04%
SINE	0.64%
LTR	25.53%
retrotransposons	
DNA transposons	12.67%
Unclassified	3.99%
Total	47.87%

LTR types	Proportion
Ty3/Gypsy	40.75%
Ty1/Copia	23.88%
Other	35.37%

Supplementary Table 6. Telomere scaffolds

Scaffold name	Scaffold length	Repeat start	Repeat end	Number of copies	Length from end of scaffold
Scaffold 1	87,013,940	86,974,270	86,992,249	2,547	21,691
Scaffold 8	46,631,104	46,616,307	46,628,952	1,801	2,152
Scaffold 13	4,922,974	4,772,062	4,792,208	2,821	130,766
Scaffold 867	17,896	1,445	17,896	2,355	0
Scaffold 901	17,187	11,108	17,187	868	0
Scaffold 1469	9,273	5,178	7,433	320	1,840

Supplementary Table 7. Distribution of NUPT lengths identified from the SCT nuclear genome

Scaffold no.	Length (bp)
1	85,208
2	106,958
3	78,893
4	61,608
5	67,435
6	55,275
7	43,295
8	43,134
9	37,243
10	37,481
11	32,187
12	38,239
Total	686,956
Mean	57,246

Supplementary Table 8. Distribution of NUPT lengths identified from the SCT nuclear genome

NUPT length (bp)	No. of NUPT	Cumulative %	Sum of NUPT length (bp)
> 5000	1	100	20,628
3500–5000	1	99.97	4,329
2000–3499	2	99.94	5,116
1000–1999	21	99.88	27,100
500–999	96	99.26	59,990
250–499	674	96.43	222,391
< 250	2,593	76.53	347,402
Total	3,388		686,956

Supplementary Table 9. Increased or reduced protein family domains (Pfam) in SCT

Supplementary Table 9 is an Excel file.

Supplementary Table 10. Enriched gene ontology (GO) terms of SCT's expanded gene families

Supplementary Table 10 is an Excel file. Enrichment was calculated by TopGO⁷

Supplementary Table 11. Enriched gene ontology (GO) terms of SCT's contracted gene families

Supplementary Table 11 is an Excel file. Enrichment was calculated by TopGO⁷

Supplementary Table 12. *CkTPS* organization of six TPS subfamilies

	TPS-a	TPS-b	TPS-c	TPS-e	TPS-f	TPS-g	Total
Scaffold 1	1	0	2	0	0	0	3
Scaffold 2	5	5	0	0	1	0	11
Scaffold 3	0	2	0	0	0	0	2
Scaffold 4	0	5	0	0	0	0	5
Scaffold 5	0	0	0	0	0	0	0
Scaffold 6	0	1	0	0	0	0	1
Scaffold 7	8	12	0	5	3	1	29
Scaffold 8	0	0	0	0	0	0	0
Scaffold 9	0	0	0	0	0	0	0
Scaffold 10	7	11	0	0	0	2	19
Scaffold 11	3	3	0	0	0	0	3
Scaffold 12	0	0	0	0	3	0	3
Scaffold others	1	22	0	0	0	1	24
Total	25	58	2	5	7	4	101

Supplementary Table 13. Examination of positive selection on the branches leading to the two TPS-f Lau clades using the branch-site model test¹.

Branch ²	Model	-lnL	2δ(lnL)	P value	ω value	Positively selected sites ³
TPS-f-Lau I	Null	32227.431			ω0 = 0.199, ω1 = 1, ω2 = 1	
	Alternative	32216.050	22.762	0.00001	ω0 = 0.201, ω1 = 1, ω2 = 894.197	403 W (0.959)
TPS-f-Lau II	Null	32232.241			ω0 = 0.205, ω1 = 1, ω2 = 1	
	Alternative	32228.503	7.476	0.006253	ω0 = 0.204, ω1 = 1, ω2 = 998.994	None

¹This analysis was based on the tree topology of Supplementary Fig. 24. We used the Codeml program of PAML⁸ to compare the null model (model = 2, Nsites =2, fixed omega = 1, omega =1) with the alternative model (model = 2, Nsites = 2, fixed omega = 0, omega = 1) in either four members of TPS-f Lau I clade or five members of TPS-f Lau II clade against all members plus the 12 non-magnoliids sequences (n=21). Four categories of sites were assumed⁹. They were (1) sites under purifying selection ($\omega_0 < 1$) on both foreground and background branches, (2) sites under neutral selection ($\omega_0 = 1$) on both foreground and background branches, (3) sites under positive selection ($\omega_2 > 1$) on the foreground branch and under purifying selection ($\omega_0 < 1$) on background branches, and (4) sites under positive selection ($\omega_2 > 1$) on the foreground branch and under neutral evolution ($\omega_1 = 1$) on background branches. In the null model, ω_2 was fixed at 1.

²The examined branches are denoted by a circle in Supplementary Fig. 27.

³The position in the multiple sequence alignment and its amino acid residue are shown. The value inside the parenthesis is the posterior probability under Bayes empirical Bayes analysis.

References

- 1 Haas, B. J., Delcher, A. L., Wortman, J. R. & Salzberg, S. L. DAGchainer: a tool for mining segmental genome duplications and synteny. *Bioinformatics (Oxford, England)* **20**, 3643-3646, doi:10.1093/bioinformatics/bth397 (2004).
- 2 Quinlan, A. R. & Hall, I. M. BEDTools: a flexible suite of utilities for comparing genomic features. *Bioinformatics (Oxford, England)* **26**, 841-842, doi:10.1093/bioinformatics/btq033 (2010).
- 3 Vurture, G. W. *et al.* GenomeScope: fast reference-free genome profiling from short reads. *Bioinformatics* **33**, 2202-2204, doi:10.1093/bioinformatics/btx153 (2017).
- 4 Mirarab, S. & Warnow, T. ASTRAL-II: coalescent-based species tree estimation with many hundreds of taxa and thousands of genes. *Bioinformatics* **31**, i44-52, doi:10.1093/bioinformatics/btv234 (2015).
- 5 Matasci, N. *et al.* Data access for the 1,000 Plants (1KP) project. *Gigascience* **3**, 17, doi:10.1186/2047-217X-3-17 (2014).
- 6 Stamatakis, A. RAxML-VI-HPC: maximum likelihood-based phylogenetic analyses with thousands of taxa and mixed models. *Bioinformatics (Oxford, England)* **22**, 2688-2690, doi:10.1093/bioinformatics/btl446 (2006).
- 7 A, A. & J, R. topGO: Enrichment Analysis for Gene Ontology. *R package version 2.26.0* (2016).
- 8 Yang, Z. PAML 4: phylogenetic analysis by maximum likelihood. *Mol Biol Evol* **24**, 1586-1591, doi:10.1093/molbev/msm088 (2007).
- 9 Zhang, J., Nielsen, R. & Yang, Z. Evaluation of an improved branch-site likelihood method for detecting positive selection at the molecular level. *Mol Biol Evol* **22**, 2472-2479, doi:10.1093/molbev/msi237 (2005).